Hindawi
Modelling and Simulation in Engineering
Volume 2018, Article ID 2945325, 12 pages
https://doi.org/10.1155/2018/2945325

Research Article

Turbogenerator Steam Turbine Variation in Developed Power: Analysis of Exergy Efficiency and Exergy Destruction Change

Vedran Mrzljak, Tomislav Senčić, and Božica Žarković

Faculty of Engineering, University of Rijeka, Vukovarska 58, 51000 Rijeka, Croatia

Correspondence should be addressed to Vedran Mrzljak; vedran.mrzljak@riteh.hr

Received 2 December 2017; Revised 17 April 2018; Accepted 18 April 2018; Published 2 July 2018

Academic Editor: Azah Mohamed

Developed power variation of turbogenerator (TG) steam turbine, which operates at the conventional LNG carrier, allows insight into the change in turbine exergy efficiency and exergy destruction during the increase in turbine power. Measurements of required operating parameters were performed in eight different TG steam turbine operating points during exploitation. Turbine exergy efficiency increases from turbine power of 500 kW up to 2700 kW, and maximum exergy efficiency was obtained at 70.13% of maximum turbine developed power (at 2700 kW) in each operating point. From turbine developed power of 2700 kW until the maximum power of 3850 kW, exergy efficiency decreases. Obtained change in TG turbine exergy efficiency is caused by an uneven intensity of increase in turbine developed power and steam mass flow through the turbine. TG steam turbine exergy destruction change is directly proportional to turbine load and to steam mass flow through the turbine—higher steam mass flow results in a higher turbine load which leads to the higher exergy destruction and vice versa. The higher share of turbine developed power and the lower share of turbine exergy destruction in the TG turbine exergy power inlet lead to higher turbine exergy efficiencies. At each observed operating point, turbine exergy efficiency in exploitation is lower when compared to the maximum obtained one for 8.39% to 12.03%.

1. Introduction

Marine propulsion systems nowadays are usually based on diesel engines [1]. Because of their wide usage, a lot of simulation and optimization numerical models were developed [2, 3] in order to investigate their operating parameters. Today, researchers are intensively involved in the investigation of alternative fuels for diesel engines [4] with the goal of reducing their emissions [5].

Unlike the rest of the world fleet, the dominant type of propulsion for LNG carriers of any kind is steam propulsion due to the specificity of their operation and the transported cargo [6]. The structure of marine steam propulsion system does not differ greatly in comparison with land-based steam power systems [7], but some of its components and the principle of operation can significantly vary.

Steam propulsion system on the LNG carrier always consists of two steam generators [8] due to safety and reliable operation. Those steam generators have burners which can operate with two fuels simultaneously—with evaporated natural gas from cargo tanks and with heavy fuel oil, so its operation dynamics differ greatly when compared to industrial scale furnaces [9]. Each steam generator has an air heater where the air is heated with a steam because flue gasses from marine steam generators do not have high enough temperature for additional heating purposes.

The propulsion propeller drive is ensured with the main propulsion turbine [10]. Steam propulsion systems on the LNG carriers have at least two turbogenerator sets (turbogenerator sets consist of a low-power steam turbine, which drives an electric generator), and both turbogenerators operate in parallel [11]. Turbogenerator sets are designed to cover all ship requirements for electrical power, and its parallel operation ensures that ship electrical network has always at disposal enough electrical power, because safe navigation always has a priority. One such TG steam turbine

is analyzed in this paper from the aspect of exergy efficiency and exergy power losses (exergy destruction) during the increase in turbine developed power. Along with the main propulsion turbine and two turbogenerator steam turbines, the majority of steam propulsion systems on LNG carriers have also one low-power steam turbine for the main feedwater pump drive, as can be found in several land-based steam power systems [12, 13]. Low-power steam turbine for the main feedwater pump drive is backpressure steam turbine—steam after expansion in this turbine is used in some other marine steam system components. After expansion in the main propulsion turbine and turbogenerators, steam was led to the main marine condenser on liquefaction. Main marine condenser operation differs greatly in comparison with main condensers from land-based steam power systems [14], because cooling water (sea) is brought to a main marine steam condenser with pumps at low system loads after which follows a sea accumulation system (scoop) at high steam system loads.

Condensate and feedwater return channel from the main marine condenser to steam generators has several devices which provide water heating. The first of such devices after the main condenser is evaporator (freshwater generator) [15], the marine steam system component which is not required in land-based steam power systems. After evaporator is located sealing steam condenser [16] and usually two condensate and feedwater heaters (low-pressure condensate heater [17] before deaerator and high-pressure feedwater heater [18] after deaerator). In comparison with land-based steam power systems, marine steam system has always much lower number of condensate and feedwater heaters, because of limited ship space. On water return channel is also mounted hot well for collecting all the condensate from the system. Condensate and feedwater heating system in land-based steam power systems as well as in marine steam propulsion systems is the most appropriate for various improvements [19] and optimizations [20] in order to reduce fuel consumption and thus emissions from steam generators [21]. New investigations for improving heat transfer as reported in [22] or [23] can surely be applied in marine steam propulsion systems at several heat exchangers, not only at condensate and feedwater heaters.

The analyzed LNG carrier has two identical turbogenerator sets that operate in parallel. Each TG steam turbine has identical operating parameters (inlet and outlet steam temperatures, pressures, and mass flows) and for the analysis in this paper is selected one of them. Steam turbine for each electric generator drive comprises nine Rateau stages. Steam turbines with Rateau stages and their analysis can be found in [24]. Many details of the classic and special designs of marine steam turbines and their auxiliary systems are presented in [25] and [26].

The main goal of this analysis was to obtain the optimal operating area of the TG steam turbine in which will be achieved maximum exergy efficiencies and minimum exergy destructions, for every turbine operating point. As a known parameter is taken a TG turbine developed power which was varied from 500 kW up to maximum turbine developed power of 3850 kW in steps of 100 kW. For each TG turbine developed power, turbine exergy efficiency and exergy destruction were calculated. Obtained areas of turbine maximum exergy efficiency and minimum exergy destruction were compared with the real LNG carrier exploitation (according to measured operating parameters). The main conclusion of TG steam turbine exergy analysis is that, in exploitation, turbine should be more loaded to obtain higher exergy efficiency in each operating point, but it would not be advisable that turbine operates at maximum load (at 3850 kW). TG turbine exergy destruction change does not follow the exergy efficiency trends, so from the viewpoint of turbine exergy destruction, it would not be advisable that turbine operates in the same operating areas as for maximum exergy efficiency. The distribution of TG steam turbine exergy power inlet shows that the higher share of turbine developed power and the lower share of turbine exergy destruction in exergy power inlet lead to higher turbine exergy efficiencies.

Table 1: Main characteristics of the LNG carrier.

Deadweight tonnage	84.812 DWT
Overall length	288 m
Maximum breadth	44 m
Design draft	9.3 m
Steam generators	2 × Mitsubishi MB-4E-KS
Propulsion turbine	Mitsubishi MS40-2 (maximum power 29.420 kW)
Turbogenerators	2 × Shinko RGA 92-2 (maximum power 3.850 kW each)

Main characteristics of the LNG carrier in which steam propulsion system is mounted analyzed turbogenerator steam turbine are presented in Table 1.

2. TG Steam Turbine Exergy Analysis

2.1. Equations for the Exergy Analysis. Exergy analysis is based on the second law of thermodynamics [27]. The main exergy balance equation for a standard volume in steady state is [28, 29]

$$\dot{X}_{\text{heat}} - P = \sum \dot{m}_{\text{OUT}} \cdot \varepsilon_{\text{OUT}} - \sum \dot{m}_{\text{IN}} \cdot \varepsilon_{\text{IN}} + \dot{E}_{\text{ex,D}}, \quad (1)$$

where the net exergy transfer by heat ($\dot{X}_{\text{heat}}$) at the temperature T is equal to [30]

$$\dot{X}_{\text{heat}} = \sum \left(1 - \frac{T_0}{T}\right) \cdot \dot{Q}. \quad (2)$$

Specific exergy was defined according to [8, 31] by the following equation:

$$\varepsilon = (h - h_0) - T_0 \cdot (s - s_0). \quad (3)$$

The total exergy of a flow for every fluid stream can be calculated according to [11]

$$\dot{E}_{\text{ex}} = \dot{m} \cdot \varepsilon = \dot{m} \cdot [(h - h_0) - T_0 \cdot (s - s_0)]. \quad (4)$$

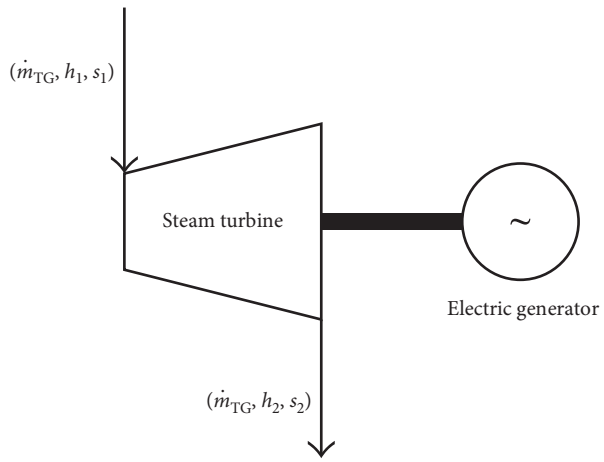

Figure 1: TG steam turbine along with main operating parameters connected to an electric generator.

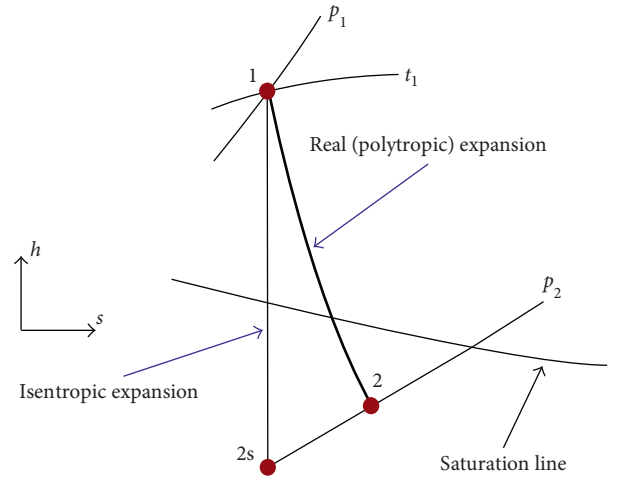

Figure 2: Steam turbine real (polytropic) and ideal (isentropic) expansion.

Exergy efficiency is also called second law efficiency or effectiveness [32]. It is defined as

$$\eta_{ex} = \frac{\text{exergy output}}{\text{exergy input}}. \tag{5}$$

2.2. Turbogenerator Turbine Exergy Efficiency and Exergy Destruction. Low-power steam turbine for electrical generator drive is condensing type and consists of nine Rateau stages [33]. Schematic view of steam turbine, which is directly connected to an electric generator, is presented in Figure 1. Steam mass flow, steam specific enthalpy, and steam specific entropy at the TG steam turbine inlet and outlet are also presented in Figure 1.

TG turbine power calculation at different loads was necessary for the TG turbine analysis. The turbine developed power in relation to steam mass flow through the turbine was approximated by the third degree polynomial by using producer data [33]:

$$P_{TG} = -4.354 \cdot 10^{-10} \cdot \dot{m}_{TG}^3 + 6.7683 \cdot 10^{-6} \cdot \dot{m}_{TG}^2 + 0.251318 \cdot \dot{m}_{TG} - 256.863, \tag{6}$$

where P_{TG} was obtained in kW when $\dot{m}_{TG}$ in kg/h was placed in (6). Steam mass flow through the TG turbine ($\dot{m}_{TG}$) was measured at each observed turbine operating point.

Steam mass flow at the TG turbine inlet is the same as steam mass flow at the TG turbine outlet because during measurements was not detected any steam leakage. The mass balance for the TG steam turbine inlet and outlet is

$$\dot{m}_{TG,1} = \dot{m}_{TG,2} = \dot{m}_{TG}. \tag{7}$$

According to Figures 1 and 2, h_1 is steam specific enthalpy at the turbine inlet and h_2 is steam specific enthalpy at the turbine outlet after real (polytropic) expansion. Complete exergy analysis of TG steam turbine is based on the real (polytropic) turbine expansion. Ideal (isentropic) expansion is presented in Figure 2 just to compare ideal steam expansion process on the turbine with the real one. Steam specific enthalpy at the turbine inlet (h_1) and steam specific entropy at the turbine inlet (s_1) were calculated from the measured pressure and temperature. Steam specific enthalpy at the turbine outlet (h_2) was calculated from the turbine power P_{TG} in kW and measured steam mass flow $\dot{m}_{TG}$ in kg/s according to [27] by using the following equation:

$$h_2 = h_1 - \frac{P_{TG}}{\dot{m}_{TG}}. \tag{8}$$

The steam specific entropy at the turbine outlet (s_2) was calculated from steam specific enthalpy at the turbine outlet (h_2) and measured pressure at the turbine outlet (p_2), as shown in Figure 2.

Steam specific enthalpy at the turbine inlet and both steam specific entropies (at the turbine inlet and outlet) were calculated by using NIST REFPROP 8.0 software [34].

TG steam turbine exergy power inlet is calculated according to [7] by using the following equation:

$$\dot{E}_{TG,ex,IN} = \dot{m}_{TG} \cdot \varepsilon_1 = \dot{m}_{TG} \cdot \varepsilon_2 + P_{TG} + \dot{E}_{TG,ex,D} = \dot{E}_{TG,ex,OUT} + \dot{E}_{TG,ex,D}, \tag{9}$$

while TG steam turbine cumulative exergy power outlet is calculated as

$$\dot{E}_{TG,ex,OUT} = \dot{m}_{TG} \cdot \varepsilon_2 + P_{TG}. \tag{10}$$

Cumulative TG steam turbine exergy power outlet consists of two parts: steam exergy power outlet and turbine developed power.

TG steam turbine exergy destruction (exergy power loss) was calculated according to [35, 36] by using the following equation:

$$\dot{E}_{TG,ex,D} = \dot{m}_{TG} \cdot \varepsilon_1 - \dot{m}_{TG} \cdot \varepsilon_2 - P_{TG} = \dot{m}_{TG} \cdot (\varepsilon_1 - \varepsilon_2) - P_{TG} = \dot{E}_{TG,ex,IN} - \dot{E}_{TG,ex,OUT}. \tag{11}$$

Steam specific exergies at the TG turbine inlet and outlet were calculated according to (3) by using calculated steam specific enthalpies and steam specific entropies at the turbine inlet and outlet.

The ambient state in the LNG carrier engine room during measurements was

Table 2: Measurement results for TG steam turbine in various operation regimes.

Operating point	Steam pressure at the TG turbine inlet (MPa)	Steam temperature at the TG turbine inlet (°C)	Steam pressure at the TG turbine outlet (MPa)	Steam mass flow through TG turbine (kg/h)
1	6.21	491.0	0.00541	4648.83
2	6.22	491.0	0.00489	4556.16
3	5.97	490.5	0.00425	4000.58
4	6.07	491.0	0.00392	3838.78
5	6.07	502.5	0.00397	3778.91
6	6.01	504.5	0.00420	4070.84
7	5.89	501.5	0.00554	4689.03
8	5.80	493.0	0.00557	4428.43

(i) pressure: $p_0 = 0.1$ MPa = 1 bar,

(ii) temperature: $T_0 = 25°C = 298.15$ K.

The exergy efficiency of a TG steam turbine was calculated according to [35, 37] by using the following equation:

$$\eta_{TG,ex} = \frac{P_{TG}}{\dot{m}_{TG} \cdot (\varepsilon_1 - \varepsilon_2)} = \frac{P_{TG}}{\dot{m}_{TG} \cdot [h_1 - h_2 - T_0 \cdot (s_1 - s_2)]}. \quad (12)$$

2.3. Developed Power Variation Principle of a TG Steam Turbine. TG steam turbine developed power can be calculated according to Figure 2 by the following equation:

$$P_{TG} = \dot{m}_{TG} \cdot (h_1 - h_2). \quad (13)$$

Three different methods can be used for the TG turbine power variation. The main assumption, valid at any TG steam turbine operating point, is always the same steam inlet pressure and temperature and the same steam outlet pressure. TG turbine power variation methods are as follows:

(1) Change in steam mass flow through the TG steam turbine

(2) Change in the value of steam specific enthalpy at the turbine outlet (h_2)

(3) Combination of methods 1 and 2.

To present the change in TG steam turbine exergy efficiency and exergy destruction in this paper is selected the combined method (method 3) for each operating point.

Turbine developed power was varied from 500 kW up to a maximum of 3850 kW in steps of 100 kW. Power change requires a change in steam mass flow through the turbine, so the adequate steam mass flow for any turbine power was calculated by using the reversed equation (6). At each operating point, steam pressure and temperature at the turbine inlet and steam pressure at the turbine outlet remain identical to the measured data. Steam specific enthalpy at the turbine outlet (h_2) was calculated for each turbine power and mass flow by using (8). Steam specific entropy at the turbine outlet (s_2) was calculated for each turbine power and mass flow by using steam specific enthalpy at the turbine outlet (h_2) and steam pressure at the turbine outlet (p_2). Change in steam specific enthalpy at the turbine outlet (h_2) and change in steam specific entropy at the turbine outlet (s_2) along with the change in steam mass flow and turbine developed power cause the change in TG steam turbine exergy efficiency and exergy destruction, (11) and (12).

Table 3: Measuring equipment for the TG steam turbine.

Steam temperature (TG inlet)	Greisinger GTF 601-Pt100—immersion probe [38]
Steam pressure (TG inlet)	Yamatake JTG980A—pressure transmitter [39]
Steam pressure (TG outlet)	Yamatake JTD910A—differential pressure transmitter [40]
Steam mass flow (TG inlet)	Yamatake JTD960A—differential pressure transmitter [40]

3. Measurement Results and Measuring Equipment of the Analyzed TG Steam Turbine

Measurement results of required operating parameters for TG turbine are presented in Table 2. Operating points in Table 2 presented LNG carrier steam system load (1 is the lowest system load, and 8 is the highest system load). TG steam turbine developed power does not depend on steam propulsion system load, and it depends only on the inclusion or exclusion of ship electrical consumers. Inclusion of the new electrical consumer or more of them will increase the TG steam turbine developed power and vice versa.

All the measurement results were obtained from the existing measuring equipment mounted on the TG turbine inlet and outlet. List of all used measuring equipment is presented in Table 3.

4. Exergy Efficiency and Exergy Destruction Change during Developed Power Variation of a TG Turbine

Change in TG steam turbine exergy efficiency and exergy destruction during the turbine developed power variation was presented in three operating points from Table 2—operating points 3, 5, and 8. Obtained conclusions from these three TG steam turbine operating points are also valid in all the other turbine operating points.

4.1. TG Turbine Developed Power Variation—Operating Point 3. TG steam turbine exergy efficiency change in operating point 3 (Table 2), during the developed power

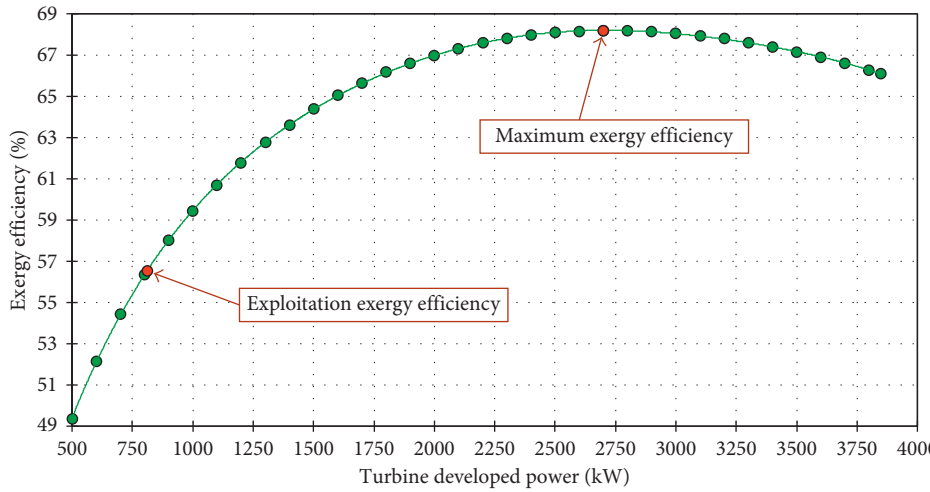

Figure 3: Steam turbine exergy efficiency change during the developed power variation—operating point 3.

variation, is shown in Figure 3. Increase in turbine developed power firstly causes an increase in exergy efficiency until the maximum value, after which follows a decrease in turbine exergy efficiency. Maximum turbine exergy efficiency is obtained at power of 2700 kW (70.13% of maximum turbine power) and amounts 68.18%. In this operating point, at the highest turbine load of 3850 kW, exergy efficiency amounts 66.10%.

Turbine exergy efficiency in each operating point, as well as in operating point 3, is calculated by using (12). An increase in turbine developed power causes an increase in steam mass flow through the turbine, which is calculated by using the reversed equation (6) where the turbine power is known and steam mass flow is an unknown variable. An increase in turbine developed power and mass flow causes a change in steam specific enthalpy at the turbine outlet (h_2) and also a change in steam specific entropy at the turbine outlet (s_2).

The most important variables which ratio defines TG turbine exergy efficiency change are turbine power and the corresponding steam mass flow. In the turbine power range from 500 kW until the 2700 kW, turbine exergy efficiency increases because the intensity of increase in turbine developed power is higher in comparison with an increase in steam mass flow through the turbine. In the turbine power range from 2700 kW until the highest turbine load of 3850 kW, the intensity of increase in turbine power is lower in comparison with an increase in steam mass flow through the turbine, so as a result in that operating area, turbine exergy efficiency decreases.

TG steam turbine load depends on ship electrical consumers and their current needs for the electrical power. In operating point 3, TG steam turbine exergy efficiency during LNG carrier exploitation amounts only 56.87% which is the much lower exergy efficiency than the maximum one obtained for this operating point. To obtain higher turbine exergy efficiency in the exploitation, the TG steam turbine should be more loaded, but not more than 2700 kW.

TG steam turbine exergy destruction is calculated by using (11) for each observed operating point. Turbine exergy destruction is the most influenced by steam mass flow through the turbine. Even a small increase in steam mass flow significantly increases the result of an (11). An increase in turbine developed power has much lower influence on the turbine exergy destruction change in comparison with the increase in steam mass flow. Continuous increase in steam mass flow during the TG turbine developed power increase from 500 kW to 3850 kW causes a continuous increase in turbine exergy destruction, as presented in Figure 4. This conclusion is valid not only in operating point 3 but also in all the other TG turbine operating points.

During LNG carrier exploitation in operating point 3, TG steam turbine exergy destruction amounts 628.82 kW, while at TG turbine maximum exergy efficiency in this operating point (at turbine developed power of 2700 kW), turbine exergy destruction amounts 1259.82 kW. At maximum turbine power of 3850 kW, exergy destruction is the highest and amounts 1974.62 kW.

TG steam turbine developed power variation showed that exergy destruction is not proportional to the turbine exergy efficiency but is directly proportional to turbine load—higher turbine load results in the higher exergy destruction and vice versa.

Analyzed TG steam turbine exergy power inlet can be presented as a sum of a turbine developed power, steam exergy power at the turbine outlet, and turbine exergy destruction, (9). It is interesting to present and compare such distribution of the exergy power inlet at two steam turbine operating phases for TG steam turbine operating point 3: first is a phase of exploitation and the second is a phase at which turbine obtained maximum exergy efficiency, Figure 3.

For TG steam turbine operating point 3, steam exergy power at the turbine outlet takes a very low share in the exergy power inlet (only 4% during exploitation and 3% at a phase of maximum exergy efficiency). The most notable differences between the phases of exploitation and maximum exergy efficiency can be seen in shares of turbine developed power and exergy destruction in the exergy power inlet. During exploitation, the share of turbine developed

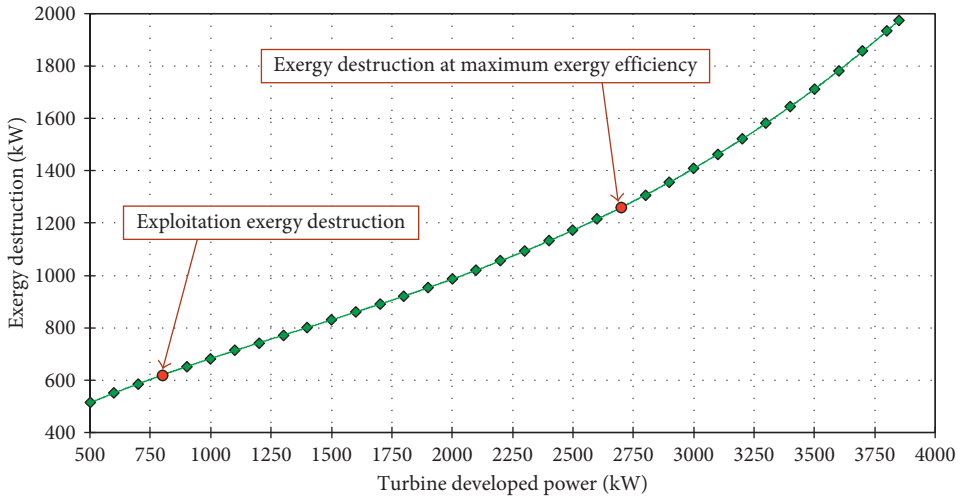

Figure 4: Steam turbine exergy destruction change during the developed power variation—operating point 3.

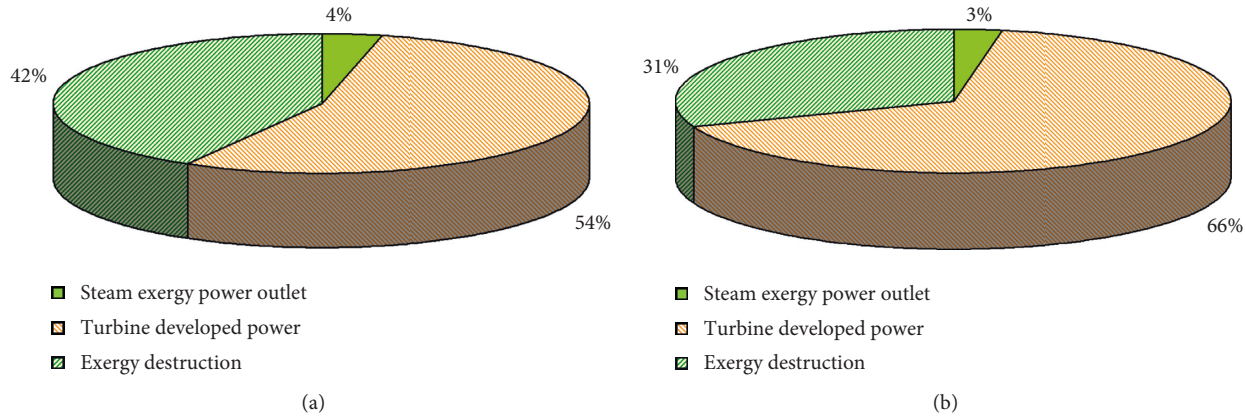

Figure 5: Distribution of steam turbine exergy power inlet for operating point 3 in exploitation (a) and at the maximum exergy efficiency (b).

power in the exergy power inlet is 12% lower, while the share of exergy destruction in the exergy power inlet is 11% higher in comparison with a phase of maximum exergy efficiency, Figure 5.

Clearly, it can be concluded that the higher share of turbine developed power and the lower share of turbine exergy destruction in the exergy power inlet lead to higher turbine exergy efficiencies. The influence of steam exergy power at the turbine outlet on the turbine exergy efficiency is negligible.

4.2. TG Turbine Developed Power Variation—Operating Point 5. Change in exergy efficiency of TG turbine in operating point 5 (Table 2), during the developed power variation, is shown in Figure 6. As in previous operating point, an increase in turbine developed power causes an increase in exergy efficiency until the maximum value, after which follows a decrease in turbine exergy efficiency.

In operating point 5, maximum turbine exergy efficiency is also obtained at developed power of 2700 kW and amounts 66.78%. For this operating point, at the highest turbine load of 3850 kW, exergy efficiency amounts 64.73%, while during LNG carrier exploitation turbine exergy efficiency amounts only 54.79%.

The reasons for such TG turbine exergy efficiency change in operating point 5 are identical as in operating point 3 described earlier. To obtain higher turbine exergy efficiency in the exploitation, the TG steam turbine should be more loaded also in observed operating point 5, but the turbine load must not exceed the value of 2700 kW.

Continuous increase in steam mass flow during the TG turbine power increase from 500 kW to 3850 kW causes a continuous increase in turbine exergy destruction, as presented in Figure 7, also at a TG turbine operating point 5. As before, steam mass flow is a dominant factor which defines the change in TG steam turbine exergy destruction.

TG steam turbine exergy destruction during LNG carrier exploitation in operating point 5 amounts 632.21 kW. At maximum exergy efficiency (2700 kW) in this operating point, the turbine exergy destruction amounts 1343.09 kW, while at maximum turbine power of 3850 kW exergy destruction is the highest and amounts 2097.61 kW.

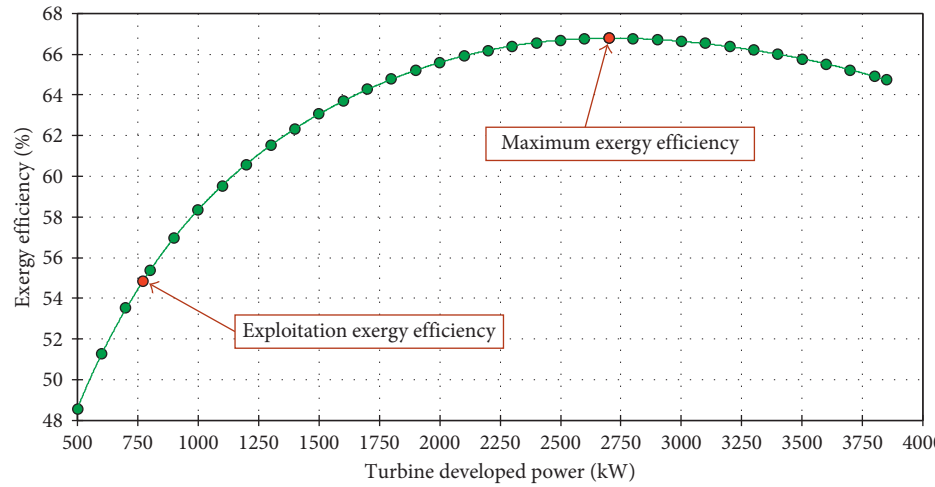

Figure 6: Steam turbine exergy efficiency change during the developed power variation—operating point 5.

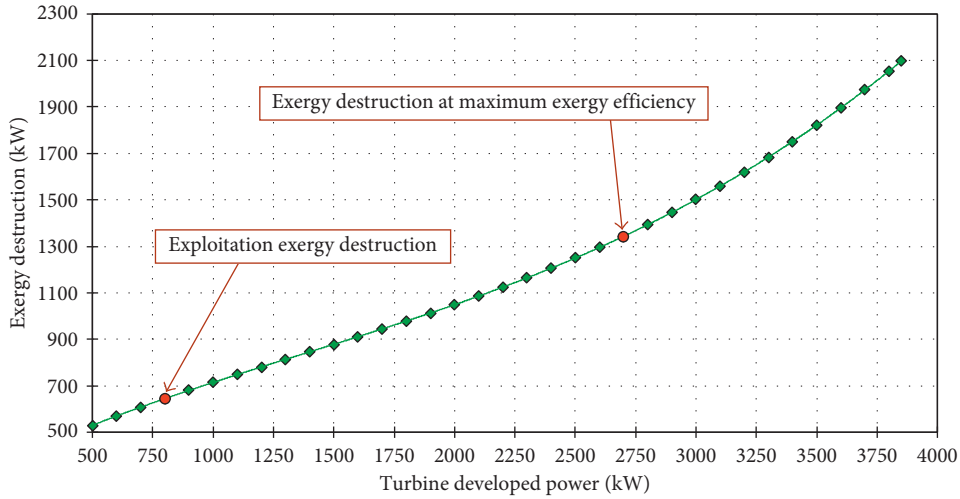

Figure 7: Steam turbine exergy destruction change during the developed power variation—operating point 5.

As in TG turbine operating point 3, exergy destruction in operating point 5 is directly proportional to turbine load—higher load results in the higher exergy destruction and vice versa.

At turbine operating point 5, steam exergy power at the turbine outlet takes a share in the exergy power inlet lower than in operating point 3 analyzed before (only 3% during exploitation and 2% at a phase of maximum exergy efficiency). Again, the most notable differences between the phases of exploitation and maximum exergy efficiency are obtained in the shares of turbine developed power and exergy destruction in the exergy power inlet, Figure 8. During exploitation at TG steam turbine operating point 5, the share of turbine developed power in the exergy power inlet is 13% lower, while the share of exergy destruction in the exergy power inlet is 12% higher in comparison with a phase of maximum exergy efficiency.

As for turbine operating point 3, at turbine operating point 5 is also valid a conclusion that the higher share of turbine developed power and the lower share of turbine exergy destruction in the exergy power inlet lead to higher turbine exergy efficiencies.

4.3. TG Turbine Developed Power Variation—Operating Point 8. The same trends and conclusions obtained from TG steam turbine operating points 3 and 5 during turbine developed power variation are also valid for operating point 8 (Table 2). In operating point 8, maximum turbine exergy efficiency amounts 70.06% and, as before, is obtained at turbine developed power of 2700 kW. At the highest turbine load (3850 kW) in operating point 8, exergy efficiency amounts 67.94%, while during LNG carrier exploitation TG turbine exergy efficiency amounts only 60.46%, Figure 9. TG steam turbine exergy efficiency during LNG carrier exploitation is 9.6% lower than the maximum one obtained in operating point 8.

TG turbine operating point 8 also confirmed conclusion that exergy destruction is proportional to turbine load—higher load results in the higher exergy destruction

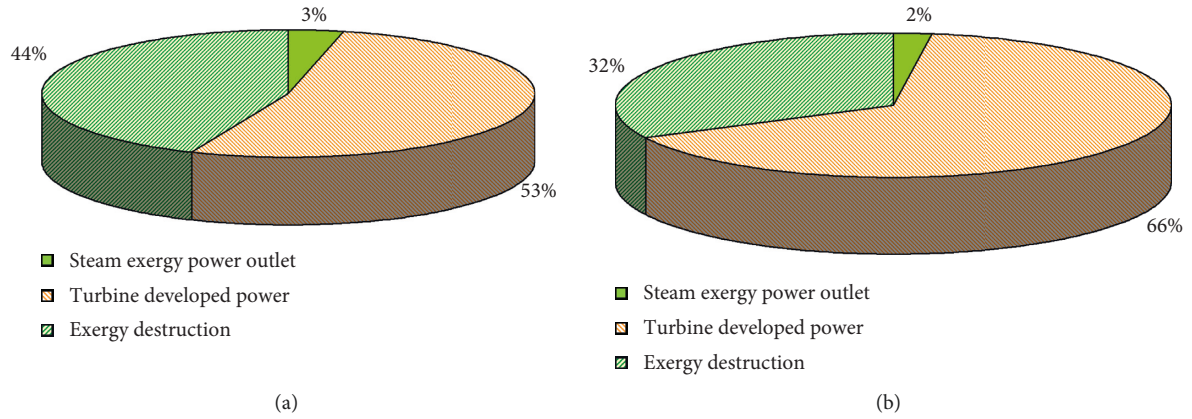

Figure 8: Distribution of steam turbine exergy power inlet for operating point 5 in exploitation (a) and at the maximum exergy efficiency (b).

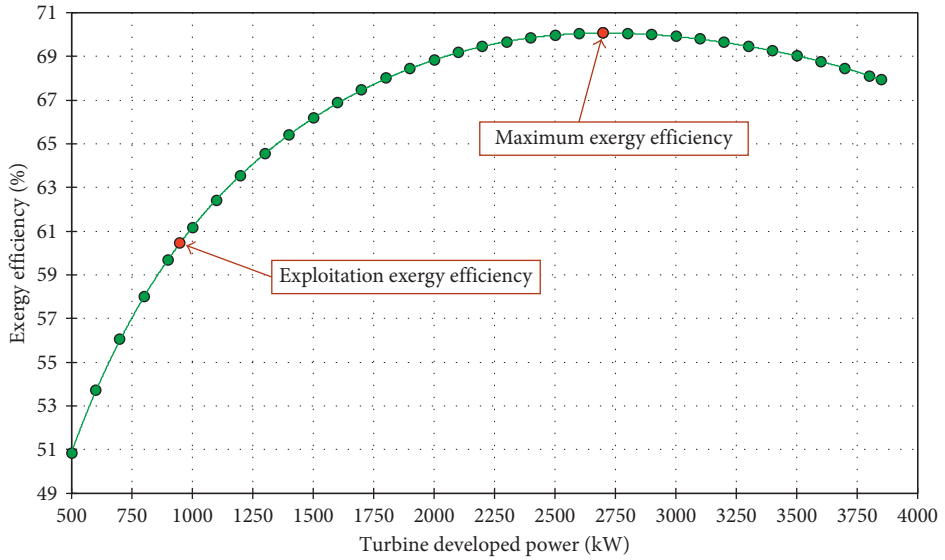

Figure 9: Steam turbine exergy efficiency change during the developed power variation—operating point 8.

and vice versa, Figure 10. In operating point 8 TG steam turbine exergy destruction during LNG carrier exploitation amounts 621.86 kW, at maximum exergy efficiency turbine exergy destruction amounts 1153.88 kW, while at maximum turbine power of 3850 kW, exergy destruction is the highest and amounts 1816.85 kW.

Steam exergy power at the turbine outlet in operating point 8 has sensibly higher share in the exergy power inlet when compared with operating points 3 and 5, and it amounts 6% in both exploitation and at maximum turbine exergy efficiency phase, Figure 11. TG steam turbine operating point 8 does not deviate when compared with operating points 3 and 5—the most notable differences between the phases of exploitation and maximum exergy efficiency can be seen in shares of turbine developed power and exergy destruction in the exergy power inlet. In a phase of maximum exergy efficiency, the share of turbine developed power in the exergy power inlet is 9% higher, while the share of exergy destruction in the exergy power inlet is 9% lower in comparison with the exploitation phase, Figure 11.

The same conclusion follows from all three analyzed turbine operating points (operating points 3, 5, and 8)—the higher share of turbine developed power and the lower share of turbine exergy destruction in the exergy power inlet lead to higher turbine exergy efficiencies and vice versa. This conclusion is also valid for all the other TG steam turbine operating points presented in Table 2.

5. Comparison of Steam Turbine Exergy Efficiency and Exergy Destruction for All Observed Operating Points (Exploitation versus Maximum Exergy Efficiency Phase)

In this section is presented a comparison of TG steam turbine exergy efficiencies and exergy destructions at two

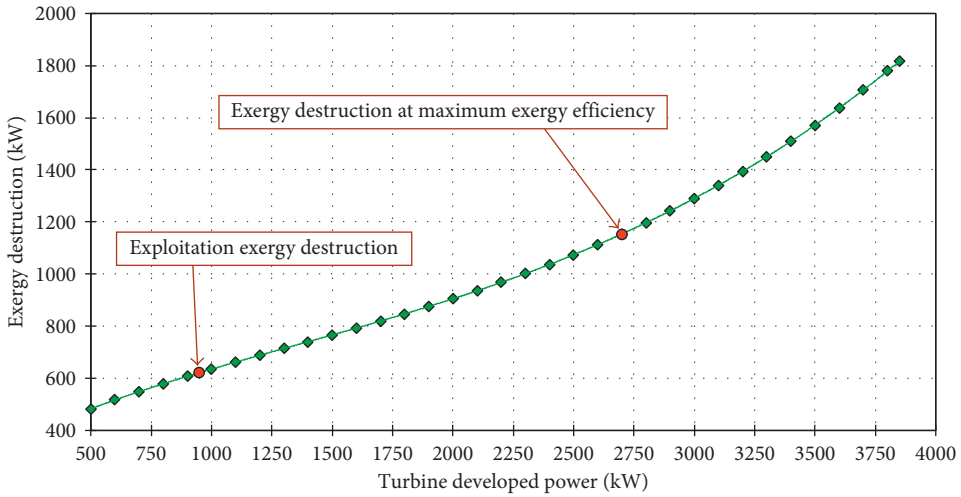

Figure 10: Steam turbine exergy destruction change during the developed power variation—operating point 8.

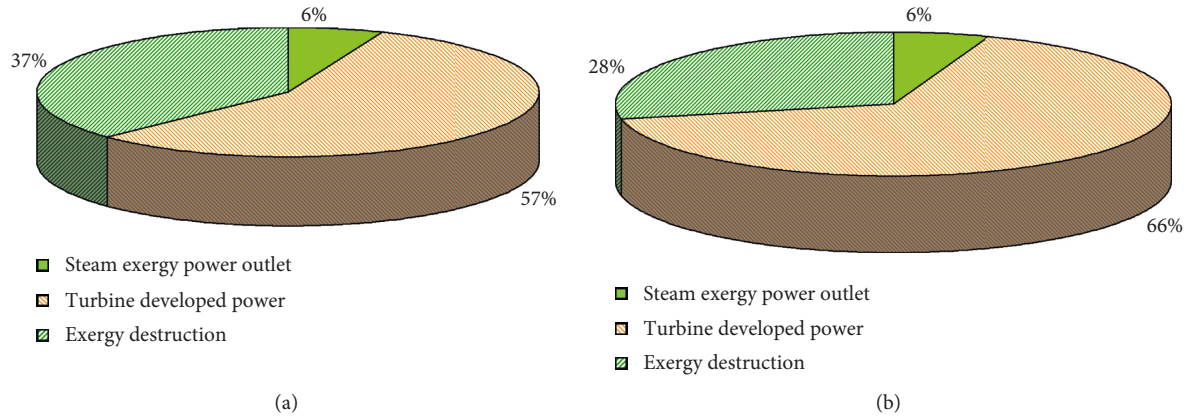

Figure 11: Distribution of steam turbine exergy power inlet for operating point 8 in exploitation (a) and at the maximum exergy efficiency (b).

operating phases—during the exploitation and during the phase of maximum exergy efficiency obtained by turbine developed power variation. The comparison is presented for all TG steam turbine analyzed operating points from Table 2.

For all observed TG steam turbine operating points is valid a conclusion that maximum turbine exergy efficiency will be obtained at turbine developed power of 2700 kW. In operating point 7, turbine exergy efficiency in exploitation is the closest to the maximum possible one and the difference is 8.39% (exploitation exergy efficiency in operating point 7 amounts 60.92% while the maximum exergy efficiency for this turbine operating point is 69.71%). For turbine operating points 4 and 5, exploitation exergy efficiencies are the farthest from the maximum obtained ones—difference is 11.99% for operating point 5 and 12.03% for operating point 4, Figure 12.

The highest turbine exergy efficiencies for exploitation are obtained in operating points 1 and 7 (60.95% for operating point 1 and 60.92% for operating point 7), while the highest turbine exergy efficiencies obtained by turbine developed power variation are 69.67% for operating point 1 and 70.06% for operating point 8.

When compared exergy destructions of TG steam turbine in all observed operating points from Table 2, it can be seen that turbine exergy destruction is much lower at the exploitation phase in comparison with the phase of maximum exergy efficiency, Figure 13.

The lowest difference in the analyzed turbine exergy destruction between exploitation and maximum exergy efficiency phase can be seen in operating point 1 and amounts 525.91 kW (at operating point 1, turbine exergy destruction in exploitation amounts 649.70 kW, while for the same operating point at a phase of maximum exergy efficiency, turbine exergy destruction amounts 1175.61 kW). The highest difference in the analyzed turbine exergy destruction between exploitation and maximum exergy efficiency phase is obtained in operating point 5 and amounts 710.88 kW, Figure 13. The average difference in turbine exergy destruction between exploitation and maximum exergy efficiency phase for all eight observed operating points amounts 604.55 kW.

The value of turbine exergy destruction is not the only variable which defines turbine exergy efficiency value. According to (12), turbine exergy efficiency is depended on the ratio of turbine developed power and turbine exergy

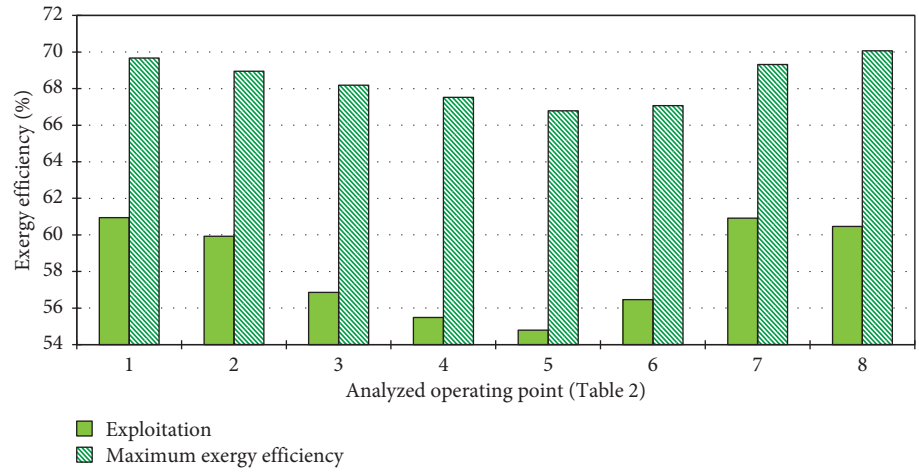

Figure 12: Comparison of exergy efficiencies for all analyzed operating points—exploitation versus maximum exergy efficiency phase.

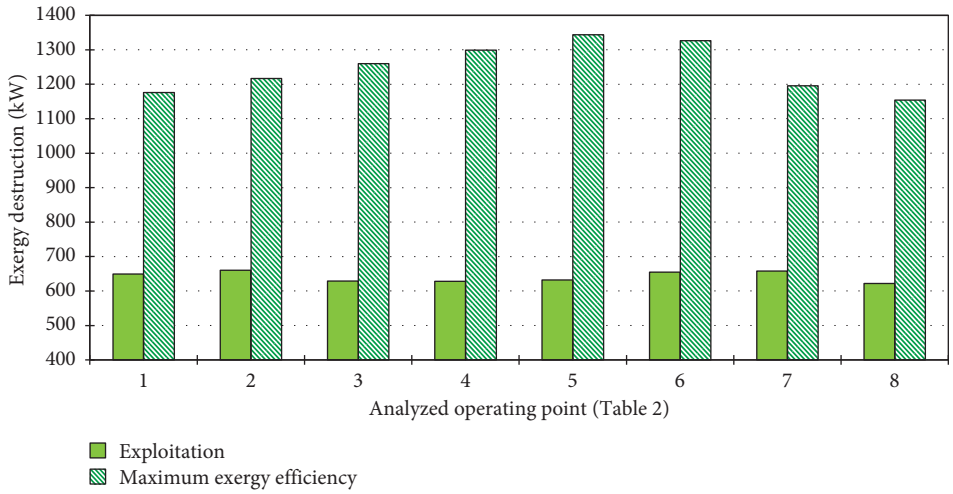

Figure 13: Comparison of exergy destructions for all analyzed operating points—exploitation versus maximum exergy efficiency phase.

destruction (turbine exergy destruction is the most influenced with a steam mass flow through the turbine). When turbine developed power increases with a higher intensity in comparison with increase in turbine exergy destruction (increase in turbine exergy destruction is proportional to increase in steam mass flow)—turbine exergy efficiency will increase. Therefore, an increase in turbine exergy destruction does not have to reduce turbine exergy efficiency simultaneously; moreover, for the analyzed TG steam turbine, increase in turbine developed power up to 2700 kW will be resulted in a simultaneous increase in turbine exergy destruction and exergy efficiency.

6. Conclusions

Numerical analysis of TG steam turbine exergy efficiency and exergy destruction (exergy power losses) change during the variation in turbine developed power was presented in this paper. TG steam turbine operates in the conventional LNG carrier steam propulsion system. Measurements were performed in eight different TG steam turbine operating points, and detailed analysis is presented for three randomly selected operating points, but major conclusions are valid for the entire TG turbine operating range.

Analyzed TG steam turbine exergy efficiency increases from 500 kW to 2700 kW of developed power, and maximum exergy efficiency was obtained at 70.13% of maximum turbine power (at 2700 kW) in each observed operating point. From 2700 kW until the maximum of 3850 kW, TG turbine exergy efficiency decreases. Increase and decrease in TG turbine exergy efficiency are caused by an uneven intensity of increase in turbine developed power and steam mass flow. The recommendation is that, in exploitation, the TG steam turbine should be more loaded to achieve higher exergy efficiency, but the turbine load must not exceed the value of 2700 kW.

TG steam turbine exergy destruction is proportional to turbine load, while turbine load is proportional to steam mass flow through the turbine—higher steam mass flow results in a higher load which leads to the higher exergy

destruction and vice versa. The lowest TG turbine exergy destruction is obtained at the lowest observed turbine load, while the highest exergy destruction is obtained at the highest turbine load in each operating point. The main reason for continuous increase in turbine exergy destruction during the developed turbine power increase is found in continuous increases in steam mass flow through the turbine. Even a small increase in steam mass flow significantly increases the turbine exergy destruction.

It was also investigated the distribution of turbine exergy power inlet for three randomly selected operating points. The major conclusion from the turbine exergy power inlet distribution analysis is that the higher share of turbine developed power and the lower share of turbine exergy destruction in the exergy power inlet lead to higher turbine exergy efficiencies and vice versa. The influence of steam exergy power at the turbine outlet on the turbine exergy efficiency change is negligible.

At each observed operating point, turbine exergy efficiency in LNG carrier exploitation is lower from 8.39% to 12.03% when compared to the maximum obtained one by this analysis. For all of the observed TG steam turbine operating points, exergy destruction in exploitation is lower between 525.91 kW and 710.88 kW in comparison with maximum exergy efficiency phase.

This analysis can be helpful to ship crew not only on the analyzed LNG carrier but also on other similar LNG carriers with similar turbogenerator units to optimize their operation and achieve the highest possible exergy efficiencies in each TG steam turbine operating point.

Nomenclature

Greek symbols

ε: Specific exergy (kJ/kg)
η: Efficiency (–)

Abbreviations

LNG: Liquefied natural gas
TG: Turbogenerator

Subscripts

0: Ambient state
D: Destruction
ex: Exergy
IN: Inlet
OUT: Outlet
$\dot{E}$: Stream flow power (kJ/s)
h: Specific enthalpy (kJ/kg)
$\dot{m}$: Mass flow rate (kg/s or kg/h)
p: Pressure (MPa)
P: Power (kJ/s)
$\dot{Q}$: Heat transfer (kJ/s)
s: Specific entropy (kJ/kg·K)
$\dot{X}_{\text{heat}}$: Heat exergy transfer (kJ/s)
T: Temperature (°C or K).

Conflicts of Interest

The authors declare that there are no conflicts of interest regarding the publication of this article.

Acknowledgments

The authors would like to extend their appreciations to the main ship-owner office for conceding measuring equipment and for all help during the exploitation measurements. This work was supported by the University of Rijeka (Contract no. 13.09.1.1.05).

References

[1] I. A. Fernández, M. R. Gómez, J. R. Gómez, and A. A. B. Insua, "Review of propulsion systems on LNG carriers," *Renewable and Sustainable Energy Reviews*, vol. 67, pp. 1395–1411, 2017.

[2] A. J. Murphy, A. J. Norman, K. Pazouki, and D. G. Trodden, "Thermodynamic simulation for the investigation of marine Diesel engines," *Ocean Engineering*, vol. 102, pp. 117–128, 2015.

[3] V. Mrzljak, V. Medica, and O. Bukovac, "Simulation of a two-stroke slow speed diesel engine using a quasi-dimensional model," *Transactions of Famena*, vol. 40, no. 2, pp. 35–44, 2016.

[4] D. Singh, K. A. Subramanian, and M. O. Garg, "Comprehensive review of combustion, performance and emissions characteristics of a compression ignition engine fueled with hydroprocessed renewable diesel," *Renewable and Sustainable Energy Reviews*, vol. 81, pp. 2947–2954, 2018.

[5] M. N. Nabi, A. Zare, F. M. Hossain, Z. D. Ristovski, and R. J. Brown, "Reductions in diesel emissions including PM and PN emissions with diesel-biodiesel blends," *Journal of Cleaner Production*, vol. 166, pp. 860–868, 2017.

[6] O. Schinas and M. Butler, "Feasibility and commercial considerations of LNG-fueled ships," *Ocean Engineering*, vol. 122, pp. 84–96, 2016.

[7] G. R. Ahmadi and D. Toghraie, "Energy and exergy analysis of Montazeri steam power plant in Iran," *Renewable and Sustainable Energy Reviews*, vol. 56, pp. 454–463, 2016.

[8] V. Mrzljak, I. Poljak, and V. Medica-Viola, "Dual fuel consumption and efficiency of marine steam generators for the propulsion of LNG carrier," *Applied Thermal Engineering*, vol. 119, pp. 331–346, 2017.

[9] E. Keshavarz, D. Toghraie, and M. Haratian, "Modeling industrial scale reaction furnace using computational fluid dynamics: a case study in Ilam gas treating plant," *Applied Thermal Engineering*, vol. 123, pp. 277–289, 2017.

[10] D. A. Taylor, *Introduction to Marine Engineering*, Elsevier Butterworth-Heinemann, Oxford, UK, 1998.

[11] V. Mrzljak, I. Poljak, and T. Mrakovčić, "Energy and exergy analysis of the turbo-generators and steam turbine for the main feed water pump drive on LNG carrier," *Energy Conversion and Management*, vol. 140, pp. 307–323, 2017.

[12] S. Adibhatla and S. C. Kaushik, "Energy and exergy analysis of a super critical thermal power plant at various load conditions under constant and pure sliding pressure operation," *Applied Thermal Engineering*, vol. 73, no. 1, pp. 51–65, 2014.

[13] S. Adibhatla and S. C. Kaushik, "Exergy and thermoeconomic analyses of 500 MWe sub critical thermal power plant with solar aided feed water heating," *Applied Thermal Engineering*, vol. 123, pp. 340–352, 2017.

[14] V. Medica-Viola, B. Pavković, and V. Mrzljak, "Numerical model for on-condition monitoring of condenser in coal-fired power plants," *International Journal of Heat and Mass Transfer*, vol. 117, pp. 912–923, 2018.

[15] M. Baawain, B. S. Choudri, M. Ahmed, and A. Purnama, *Recent Progress in Desalination, Environmental and Marine*

Outfall Systems, Springer International Publishing, Basel, Switzerland, 2015.

[16] V. Mrzljak, I. Poljak, and V. Medica-Viola, "Energy and exergy efficiency analysis of sealing steam condenser in propulsion system of LNG carrier, our sea," *International Journal of Maritime Science and Technology*, vol. 64, no. 1, pp. 20–25, 2017.

[17] V. Mrzljak, I. Poljak, and V. Medica-Viola, "Efficiency and losses analysis of low-pressure feed water heater in steam propulsion system during ship maneuvering period," *Scientific Journal of Maritime Research*, vol. 30, pp. 133–140, 2016.

[18] V. Mrzljak, I. Poljak, and V. Medica-Viola, "Thermodynamical analysis of high-pressure fed water heater in steam propulsion system during exploitation, shipbuilding: theory and practice of naval architecture," *Marine Engineering and Ocean Engineering*, vol. 68, no. 2, pp. 45–61, 2017.

[19] M. Samadifar and D. Toghraie, "Numerical simulation of heat transfer enhancement in a plate-fin heat exchanger using a new type of vortex generators," *Applied Thermal Engineering*, vol. 133, pp. 671–681, 2018.

[20] M. H. Esfe, H. Hajmohammad, D. Toghraie, H. Rostamian, O. Mahian, and S. Wongwises, "Multi-objective optimization of nanofluid flow in double tube heat exchangers for applications in energy systems," *Energy*, vol. 137, pp. 160–171, 2017.

[21] G. R. Ahmadi and D. Toghraie, "Parallel feed water heating repowering of a 200 MW steam power plant," *Journal of Power Technologies*, vol. 95, pp. 288–301, 2015.

[22] H. Kavusi and D. Toghraie, "A comprehensive study of the performance of a heat pipe by using of various nanofluids," *Advanced Powder Technology*, vol. 28, no. 11, pp. 3074–3084, 2017.

[23] A. Moraveji and D. Toghraie, "Computational fluid dynamics simulation of heat transfer and fluid flow characteristics in a vortex tube by considering the various parameters," *International Journal of Heat and Mass Transfer*, vol. 113, pp. 432–443, 2017.

[24] H. P. Bloch and M. P. Singh, *Steam Turbines-Design, Applications and Re-Rating*, The McGraw- Hill Companies, Inc., New York, NY, USA, 2nd edition, 2009.

[25] F. Baldi, F. Ahlgren, F. Melino, C. Gabrielii, and K. Andersson, "Optimal load allocation of complex ship power plants," *Energy Conversion and Management*, vol. 124, pp. 344–356, 2016.

[26] F. Haglind, "Variable geometry gas turbines for improving the part-load performance of marine combined cycles-combined cycle performance," *Applied Thermal Engineering*, vol. 31, no. 4, pp. 467–476, 2011.

[27] M. Kanoğlu, Y. A. Çengel, and I. Dincer, "Efficiency evaluation of energy systems," in *Springer Briefs in Energy*, Springer, Berlin, Germany, 2012.

[28] F. K. Zisopoulos, S. N. Moejes, F. J. Rossier-Miranda, A. J. Van der Goot, and R. M. Boom, "Exergetic comparison of food waste valorization in industrial bread production," *Energy*, vol. 82, pp. 640–649, 2015.

[29] N. Nazari, P. Heidarnejad, and S. Porkhial, "Multi-objective optimization of a combined steam-organic Rankine cycle based on exergy and exergo-economic analysis for waste heat recovery application," *Energy Conversion and Management*, vol. 127, pp. 366–379, 2016.

[30] G. Ahmadi, D. Toghraie, A. Azimian, and O. Ali Akbari, "Evaluation of synchronous execution of full repowering and solar assisting in a 200 MW steam power plant, a case study," *Applied Thermal Engineering*, vol. 112, pp. 111–123, 2017.

[31] G. Ahmadi, D. Toghraie, and O. Ali Akbari, "Solar parallel feed water heating repowering of a steam power plant: a case study in Iran," *Renewable and Sustainable Energy Reviews*, vol. 77, pp. 474–485, 2017.

[32] J. Szargut, *Exergy Method-Technical and Ecological Applications*, WIT Press, Ashurst, UK, 2005.

[33] Shinko Ind. Ltd., *Final Drawing for Generator Turbine*, Shinko Ind. Ltd., Hiroshima, Japan, 2006.

[34] E. W. Lemmon, M. L. Huber, and M. O. McLinden, *NIST Reference Fluid Thermodynamic and Transport Properties-REFPROP, Version 8.0, User's Guide*, NIST, Boulder, CO, USA, 2007.

[35] H. H. Erdem, A. V. Akkaya, B. Cetin et al., "Comparative energetic and exergetic performance analyses for coal-fired thermal power plants in Turkey," *International Journal of Thermal Sciences*, vol. 48, no. 11, pp. 2179–2186, 2009.

[36] S. C. Kaushik, V. Siva Reddy, and S. K. Tyagi, "Energy and exergy analyses of thermal power plants: a review," *Renewable and Sustainable Energy Reviews*, vol. 15, no. 4, pp. 1857–1872, 2011.

[37] F. Hafdhi, T. Khir, A. Ben Yahyia, and A. Ben Brahim, "Energetic and exergetic analysis of a steam turbine power plant in an existing phosphoric acid factory," *Energy Conversion and Management*, vol. 106, pp. 1230–1241, 2015.

[38] https://www.greisinger.de.

[39] http://www.industriascontrolpro.com.

[40] http://www.krtproduct.com.